Performance Analysis of an in GaAs Based p-i-n Photodetector

Diponkar Kundu, Dilip Kumar Sarker, Md. Galib Hasan, Pallab Kanti Podder, Md. Masudur Rahman

Abstract— an InGaAs based p-i-n photodetector model is chosen in order to find out quantum efficiency, photocurrent density, and normalized frequency response with and without RC effect. Normalized frequency response is the most important factor in order to analysis the performance of p-i-n photodetector. Quantum efficiency, photocurrent density, normalized frequency response curves are obtained by formulation which is done from structure and MATLAB simulation. A relation for the fiber-to-waveguide coupling efficiency has also been used to calculate the overall quantum-efficiency of waveguide photodetector [1]. Normalized frequency response is obtained by varying value of frequency dependent transfer function of equivalent circuit model of p-i-n photodetector with frequency. For enhancing bandwidth of photodetector, the parametric values of photodetector such as reverse bias junction capacitance and resistance, has been optimized. The effect of carrier trapping at a heterointerface has also been considered to study the frequency dependence of the photocurrent at low-bias voltages [1].

Index Terms— p-i-n photodetector, quantum efficiency, photocurrent density, normalized frequency response.

I. INTRODUCTION

A p-i-n photodetector has become most important and popular in optical fiber communication. Photodetector (PD) is mainly used in optical fiber communication as receiver. It is also used for the high-speed communication, optical storage systems CD-ROM, as well as red and blue laser DVDs. Among of p-n, p-i-n, avalanche (APD) or metal-semiconductor-metal (MSM) photodetector model, we analysis the performance of p-i-n waveguide photodetector model structure. There are several reasons for choosing p-i-n waveguide photodetector model. Waveguide photodetector model is used for increasing fiber to detector coupling efficiency. Speed of response is high for p-i-n PD than p-n PD. For p-n PD, in the depletion region carrier pairs separate and drift under the influence of electric field, whereas outside this region the hole diffuses towards the

depletion region in order to be collected [7-8]. The diffusion process is very slow compared to the drift and thus limits the response of the photodiode. But in case of p-i-n photodiode, diffusion and drift process both are very fast compared to the p-n PD and for this reasons speed of response of PD is fast. APD has the random nature of the gain mechanism which gives an additional noise contribution. But in p-i-n PD, there is a little noise effect due to low gain mechanism. It is important that both bandwidth and quantum efficiency be high for high performance photodetector. The light in the guide is evanescently coupled to the absorption layer. The thin absorption layer is good for high bandwidth but then quantum efficiency is reduced. The InGaAs-absorption layer in the model is suitable for long-haul fiber-optic communication systems at the important 1.3- and 1.55- μm wavelengths. The thin absorption layer thickness is used to decrease the transit time of carriers. The carriers are nonuniformly distributed in the two-dimensional (2-D) plane, i.e., along the length and thickness of the PD. It may be mentioned here that modeling of the frequency response is very critical in such structures. Because of the thin absorption layer, it is important to include the interface trapping effect in the modeling of a heterojunction PD [1]. Two dimensional model is used to determine frequency response. Frequency response is determined from the transfer function of equivalent circuit model of InGaAs based photodetector. 3 db bandwidth obtained from normalized frequency response curve is found to be large for optical fiber communication. Photocurrent density with respect to the position from side in where light is incident, frequency and incident optical power. Photocurrent density decreases with increasing penetration depth and increases with increasing incident optical power.

II. P-I-N PHOTODETECTOR MODEL
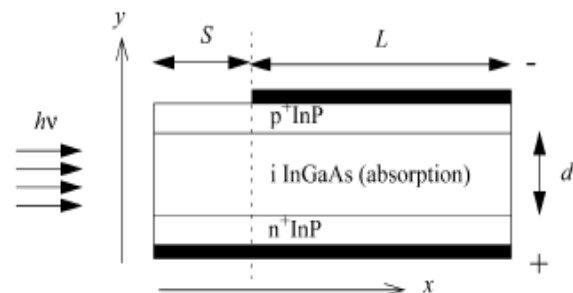
Figure 1: Schematic layer structure of a WGPD.

The InGaAs-absorption layer shown in this figure is suitable for long-haul fiber-optic communication systems at the important 1.3- and 1.55- μm wavelengths. In Fig. 1, only a part of the PD surface has contact metallization. Thus, there is no voltage applied across the front part of this layer. In some structures, the front part is made of nonabsorbent materials. This portion of the PD is called pseudo-window [1]. A pseudo-window is used to increase the device reliability [5-6]. It can be seen that for edge illumination, the photon distribution decays exponentially along the length(x) of the absorbing layer, the decay constant being determined by the absorption coefficient (α). The carriers flow along the thickness(y) of the device. So, the current is also non uniformly distributed along the x direction.
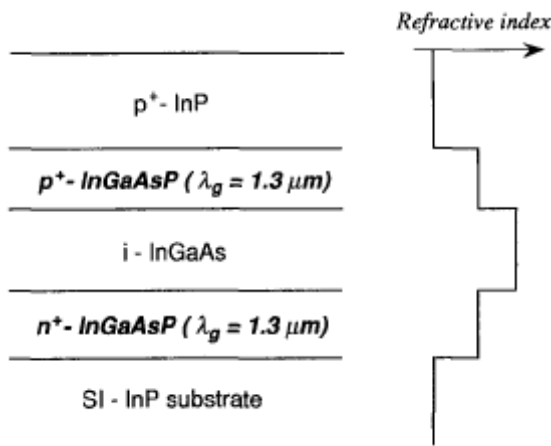
Figure 2: Epitaxial layer structure of a WGPD.

To overcome this tradeoff relationship, we have enlarged the optical field distribution at the WGPD's by adding doped intermediate band-gap layers between the InGaAs (narrow-gap) layer and InP (wide-gap) layers in figure 2. InGaAsP layers are used as the intermediate band-gap layers. These InGaAsP layers have a band-gap energy corresponding to 1.3 μm wavelength and are transparent for input light with a 1.55 μm wavelength [4]. In the calculations, it is assumed that the thickness of the upper and the lower InP cladding layers are infinite and the WGPD has a high-mesa structure which is much wider than the spot size of the input light from a hemi spherically ended fiber. Figure 2 shows a profile of the refractive index at the WGPD.

III. EQUIVALENT CIRCUIT MODEL OF P-I-N PHOTODIODE
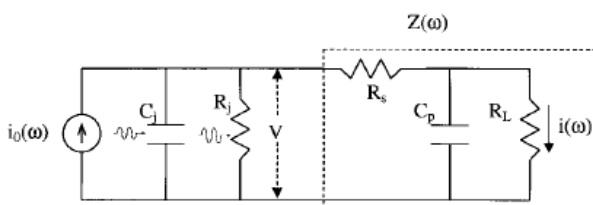
Figure 3: An equivalent circuit of a p-i-n photodiode under illumination.

An equivalent circuit of the p-i-n photodiode is shown in Fig. 3 where $i_0(w)$ represents the photocurrent at w inside the reverse-biased intrinsic region, C_j is the junction capacitance, R_j is the diode shunt junction resistance, C_p is the parasitic capacitance, R_s is the series resistance due to the contacts and the p and n regions of the diode, and R_L is the load resistor. For this circuit, the output current i(w) can be expressed as $i(w) = i_0(w)H(w)$, where H(w) is the transfer function of the circuit . The form of i(w) suggests that the harmonic distortion can manifest in $i_0(w)$ or H(w), or both. The physical origin of the nonlinearity in $i_0(w)$ and H(w) are attributed to the nonlinear carrier transport and the associated impedance changes induced by the optical input signal [3].

IV. BANDWIDTH QUANTUM EFFICIENCY PRODUCT

The overall quantum efficiency of the PD consists of many factors. An important factor in the case of a WGPD is the fiber-to-WG coupling efficiency. It depends on the geometries of the fiber as well as WG input-end, and also on the distribution of light intensity from the emitting edge of the fiber .However, for the present case we assume that the distribution is uniform. Then the coupling efficiency will be proportional to the overlapped area of the fiber cross section and the WG edge area. Assuming that the fiber and WG are very close to each other and are perfectly aligned so that the lines of symmetry are collinear, then the coupling efficiency will be a function of the distribution of emitted intensities from the fiber-end and the WG mode. So, replacing the actual thickness of the fiber by an equivalent thickness with uniform distribution, the coupling efficiency may be assumed to be approximately proportional to the overlapping area, because the overlapping area will now roughly indicate the proportion of light entering into the WG from the fiber [1]. This also simplifies the analysis that does not require the evaluation of the complex overlap integrals knowing the actual distribution of the light intensity emitted from the fiber, an equivalent area of the fiber can be calculated for the uniform intensity distribution. Thus, the present method may be applied to different light distributions.

Let us assume that the fiber diameter is D, the width of the WG is W and the thickness of the WG is d. Then, the fiber-to-WG coupling efficiency η_{f-w} is given by

$$\eta_{f-w} = 4 \frac{W}{\pi d} \sqrt{1 - \left(\frac{W}{D}\right)^2} + \frac{2}{\pi}\left[\left\{\sin^{-1}\left(\frac{d}{D}\right) + \frac{d}{D}\sqrt{1 - \left(\frac{d}{D}\right)^2}\right\} - \left\{\sin^{-1}\sqrt{1 - \left(\frac{W}{D}\right)^2} + \frac{W}{D}\sqrt{1 - \left(\frac{W}{D}\right)^2}\right\}\right]$$

……………… (1)

For d, W<D

$$\eta_{f-w} = \frac{2}{\pi}\left\{\sin^{-1}\left(\frac{d}{D}\right) + \frac{d}{D}\sqrt{1 - \left(\frac{d}{D}\right)^2}\right\}$$ ……………… (2)

For d< D and W≥ D

And when the WG edge-area is greater than fiber cross-sectional area, the coupling efficiency is unity. If the reflection coefficient R at the edge is and the absorption coefficient is (η), the quantum efficiency is given by

$$\eta = \eta_{f-w}(1-R)[1 - \exp(-\alpha L)]$$

……………… (3)

Where L is the length of the absorption layer.

V. POSITIONAL PHOTOCURRENT DENSITY

To obtain the current density, it is necessary to solve the current continuity equations. Let us consider the case of holes and assume that the holes are moving at their saturation velocity. The continuity equations are then given by

$$\frac{\delta p(x,y,t)}{\delta t} - D_p \frac{\delta^2 p(x,y,t)}{\delta x^2} = \alpha g_0 \exp(-\alpha x)\, \delta t - \frac{P(x,y,t)}{\tau_p} \quad (4)$$

And

$$\frac{\delta p(x,y,t)}{\delta t} + v_p \frac{\delta p(x,y,t)}{\delta y} - D_p \frac{\delta^2 p(x,y,t)}{\delta x^2} = \alpha g_0 \exp(-\alpha x)\, \delta(t) - \frac{P(x,y,t)}{\tau_p} \quad (5)$$

where $P(x,y,t)$ is the hole density, v_p is the saturation velocity of holes, D_p is the hole diffusion coefficient, τ_p is the recombination time-constant of holes, $g0$ is the incident photon density, δt the unit impulse function. Input intensities are assumed not to be high enough to cause saturation and the small number of photogenerated carriers is assumed to have no screening effect. These equations are solved with initial and boundary conditions. The initial condition is, $p(x,y,t) = 0$ at t=0 [2]. Let us denote the Laplace transform of $p(x,y,t)$ by $p(x,y)$ omitting the Laplace variable in the argument, for brevity. Assuming that $p(x,y) = 0$ as $x \rightarrow \infty$, then the carrier decay at x=0 is predominantly controlled by recombination, and it can be shown from (1) that

$$p(x,y) = \frac{\alpha g_0}{\alpha^2 D_p \left(s + \frac{1}{\tau_p}\right)}$$
$$\times \left[\frac{\alpha^2 D_p}{\left(s + \frac{1}{\tau_p}\right)} \exp\left(-\sqrt{\frac{\left(s + \frac{1}{\tau_p}\right)}{D_p}}\, x\right) - \exp(-\alpha x) \right] \quad \ldots\ldots(6)$$

As the carriers approach x=S where they enter into the depletion region, the electrons and holes are swept by the electric field along the direction, and thus, drift is the main mechanism for the Carrier flow in the direction. Therefore, equation (4) must be solved to obtain the current density in the PD. This equation is solved numerically by dividing L and d into a number of small segments, where d is the thickness and L is the length of the absorption layer of the PD under depletion. To obtain an approximate boundary condition at, the diffusion term in the Laplace-transformed (5) is replaced by using (6). Doing the substitution and solving for $p(x,y)$ at x=S, it can be shown that

$$P(y,t) = \frac{\alpha g_0}{\left(s + \frac{1}{\tau_p}\right)} \left[1 - \exp\left\{ -\left(s + \frac{1}{\tau_p}\right)\left(\frac{y}{v_p}\right)\right\}\right]$$
$$\times \left[\exp(-\alpha S) - \frac{\alpha^2 D_p}{\alpha^2 D_p - \left(s + \frac{1}{\tau_p}\right)} \right.$$
$$\left. \times \left\{ \exp\left(-\sqrt{\frac{\left(s + \frac{1}{\tau_p}\right)}{D_p}}\, S\right) - \exp(-\alpha S)\right\}\right].$$
$$\ldots\ldots\ldots\ldots\ldots\ldots\ldots\ldots\ldots\ldots\ldots\ldots\ldots\ldots\ldots\ldots\ldots(7)$$

Assuming that diffusion is negligible at x=S+L, i.e., at the right-hand side of the PD, the value of $p(x,y)$ at that boundary can be obtained as

$$P(S+L, y) = \frac{\alpha g_0 \exp\{-\alpha(S+L)\}}{\left(s + \frac{1}{\tau_p}\right)}$$
$$\times \left[1 - \exp\left\{-(s + \frac{1}{\tau_p})(\frac{y}{v_p})\right\}\right] \quad \ldots\ldots\ldots\ldots (8)$$

Using (7) and (8) as the boundary conditions, the Laplace transformed is numerically solved [2]. Similarly we can also be solved. Then the current density in the frequency domain can be calculated taking the integration over the thickness as shown below [2]

$$J(j\omega)=$$
$$\frac{q p_i}{\varepsilon_p x_a} \left[\frac{v_h \varepsilon_{ho}}{\varepsilon_{ho} + \varepsilon_{rh} + j\omega} \left\{ (\eta_b - \right.\right.$$
$$\eta_f \exp[-\alpha x]) \left(\frac{1 - \exp[-j\omega x_a \cdot v_h]}{j\omega}\right) + \frac{v_h \eta_f}{\alpha v_h + j\omega}\left(1 - \right.$$
$$\exp\left[-\alpha x_a - j\omega \frac{x_a}{v_h}\right]) + \frac{\eta_b v_h}{\alpha v_h - j\omega}(\exp[-\alpha x_a] - $$
$$\exp\left[-j\omega x_a / v_h\right])\right\} + \frac{v_e \varepsilon_{eo}}{\varepsilon_{eo} + \varepsilon_{re} + j\omega}\left\{ (\eta_f - \eta_b \exp[-\alpha \right.$$
$$x]) \left(\frac{1 - \exp[-j\omega x_a \cdot v_e]}{j\omega}\right) + \frac{v_e \eta_b}{\alpha v_h + j\omega}\left(1 - \exp\left[-\alpha x_a - \right.$$
$$j\omega \frac{x_a}{v_e}\right]) + \frac{\eta_f v_e}{\alpha v_h - j\omega}(\exp[-\alpha x_a] - \exp[-j\omega x_a / v_e])\right\}\right]$$

$$\ldots\ldots\ldots\ldots\ldots\ldots\ldots\ldots\ldots\ldots\ldots\ldots.. (9)$$

VI.   PERFORMANCE ANALYSIS
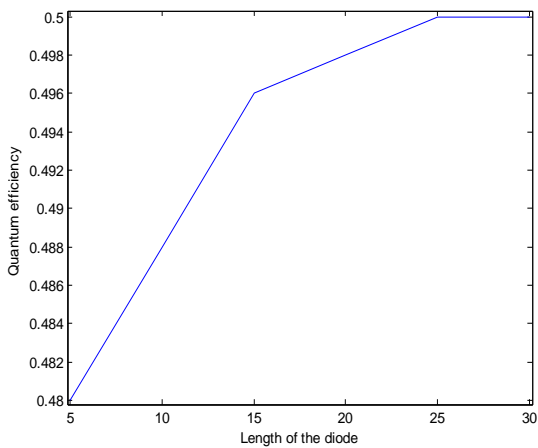
Figure 4: Quantum efficiency as function of length of the diode.
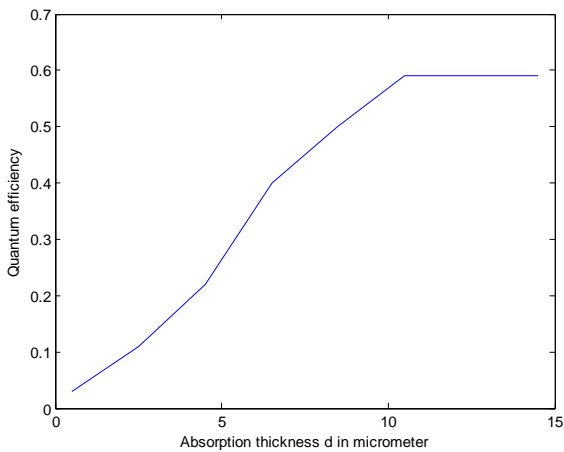
Figure 5: Quantum efficiency as a function of absorption thickness.
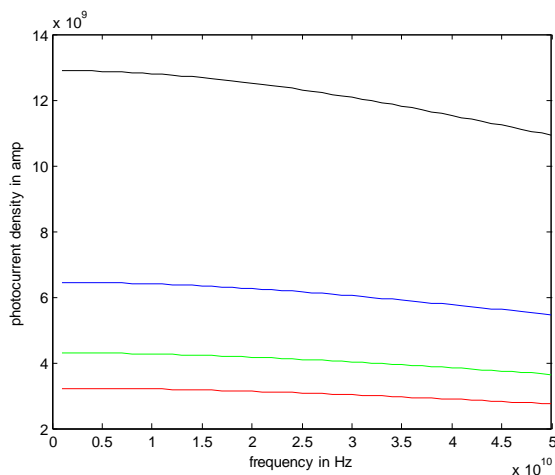
Figure 6: Photocurrent density with varying of frequency.

From this figure, it is seen that photocurrent density is decreased very sharply with increasing frequency. These curves are for different position from the surface of illumination of light. Black curve is for x=.8 μm. Blue curve is for x=1.6 μm. Green curve is for x=2.4 μm. Red curve is for x=3.2 μm. So it can say from curve photocurrent density decrease with increasing position.
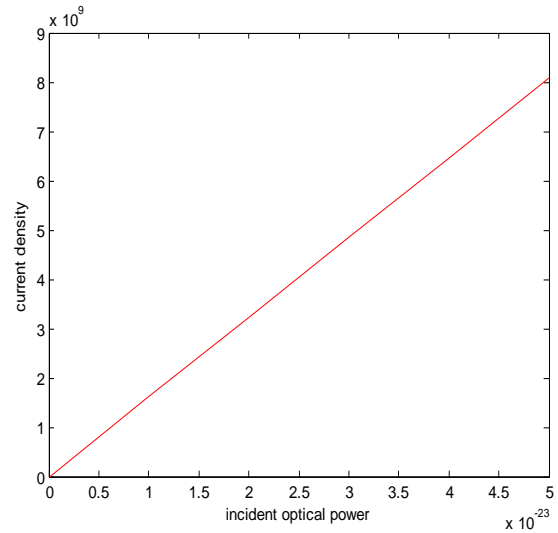
Figure 7: Photocurrent density with varying of incident optical power.

From this figure, it is seen that photocurrent density is increased linearly with increasing incident optical power.
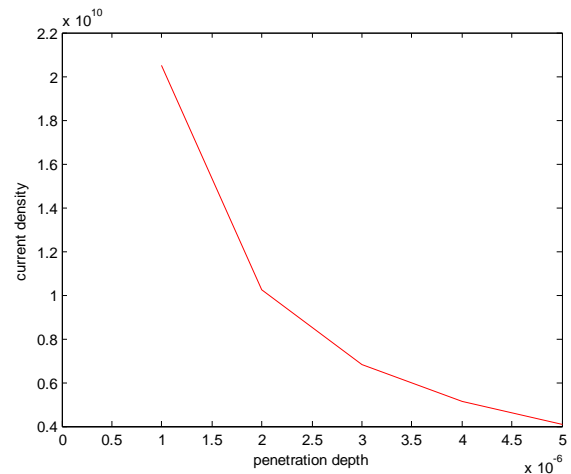
Figure 8: Photocurrent density with varying of penetration depth.

From this figure, it is seen that photocurrent density is decreased with increasing penetration depth.

Figure 9: Normalized Frequency Response With RC Effect.

From the equivalent circuit model, it is seen that there are two resistances and capacitances. One capacitance is junction capacitance and other capacitance is parasitic capacitance. One resistance is junction resistance and other resistance is series resistance due to contacts. For finding normalized frequency response, transfer function of equivalent circuit is found. All resistances and capacitances are accounted for finding transfer function. From the curve, at the 3db point, bandwidth is 40 GHz.
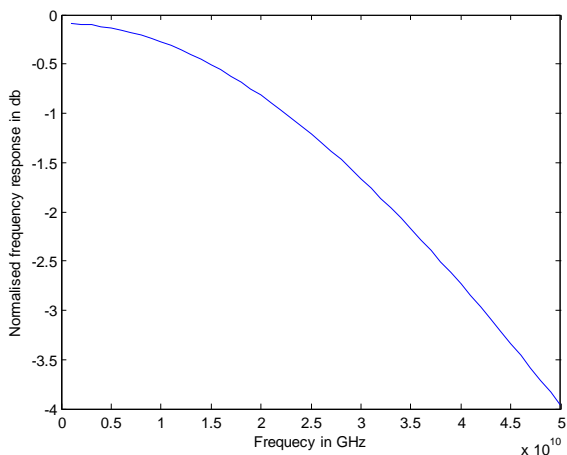
Figure 10: Normalized Frequency Response Without RC Effect.

From the equivalent circuit model, it is seen that there are two resistances and capacitances. One capacitance is junction capacitance and other capacitance is parasitic capacitance. One resistance is junction resistance and other resistance is series resistance due to contacts. For finding normalized frequency response, transfer function of equivalent circuit is found. Here only junction resistance and capacitance are accounted for finding transfer function. Series resistance and parasitic capacitance are eliminated. From the curve, at the 3db point, bandwidth is 42 GHz.

VII. CONCLUSION

The spatial 2-D distribution of carriers has been used to model the photocurrent in a WG structure of a p-i-n photodiode. It has been shown that the photocurrent density can be expressed as a function of position along the length of the device. Photocurrent density is also expressed in frequency. Photocurrent density is obtained by varying frequency at different position. Quantum efficiency curve is obtained from plotting quantum efficiency with respect to the absorption thickness. Normalized frequency curve is obtained from plotting decibel value of the transfer function of equivalent circuit model of InGaAs based p-i-n photodetector with respect to the frequency. We have evaluated 3dB bandwidth with and without RC effect. 3 db bandwidth of frequency response curve is increased by optimizing the parametric values such as reverse bias junction capacitance and resistance. When we consider RC effect then the 3dB bandwidth is 40 GHz. But if we neglect the RC effect then the 3dB bandwidth is 42 GHz. So the 3dB bandwidth without RC effect is greater than the 3dB bandwidth with RC effect. The results show that there are certain combinations of the parametric values for which normalized frequency response of the PD can be maximized.

REFERENCES

1. Nikhil Ranjan Das, Senior Member, IEEE and M. Jamal Deen, Fellow, IEEE "A Model for the Performance Analysis and Design of Waveguide p-i-n Photodetectors" IEEE Transactions on Electron Devices Vol. 53 No. 4 , April 2005.
2. Nikhil Ranjan Das, Senior Member, IEEE and M. Jamal Deen, Fellow, IEEE "Calculating the Photocurrent and Transit-Time-Limited Bandwidth of a Hetero structure p-i-n Photodetector" IEEE Journal of Quantum Electronics Vol. 37 No.12 December 2001.
3. Paul K. Yu UCSD, Jacobs School of Engineering "Equivalent Circuit Analysis of Harmonic Distortions in Photodiode" University of California Post prints 1998.
4. Kazutoshi Kato, Member, ZEEE, Susumu Hata, Kenji Kawano, Junichi Yoshida, **Senior**Member, IEEE, and Atsuo Kozen " A High-Efficiency 50 GHz InGaAs Multimode Waveguide Photodetector" IEEE Journal of Quantum Electronics Vol. 28 No.12 December 1992.
5. S. D. McDougall, M. J. Jubber, O. P. Kowalski, J. H. Marsh, and J.S. Aitchison, "GaAs/AlGaAs waveguide pin photodiodes with nonabsorbing input facets fabricated by quantum well intermixing," Electron. Lett. , vol. 36, pp. 749–750, 2000.
6. C. L. Ho, M. C. Wu, W. J. Ho, J. W. Liaw, and H. L. Wang, "Effectiveness of the Pseudowindow for edge-coupled InP-InGaAs-InP PIN photodiodes," IEEE J. Quantum Electron., vol. 36, no. 3, pp. 333–338, Mar. 2000.
7. Jasprit Singh " Optoelectronics, An Introduction To Materials And Devices" (Book)
8. John M. Senior " Optical Fiber Communication Principles and Practice" Second Edition Prentice Hall of India (Book)

AUTHOR PROFILE

First Author Diponkar Kundu received B.Sc engineering degree in the department of Electrical and Electronic Engineering department from Khulna University of Engineering and Technology on March 2009. Now he is a lecturer in the department of Electrical and Electronic Engineering of Pabna Science & Technology University, Pabna, Bangladesh. He joined as a Lecturer in the department of Electrical and Electronic Engineering Department of Pabna Science and Technology University on April 1, 2009.

Second Author Dilip Kumar Sarker was born in Rajshahi, Bangladesh in 1960. He received the B.Sc engineering degree in electrical and electronic engineering from Dhaka University of Engineering and Technology, Bangladesh in 1995 and the M.Sc engineering degree in electrical and electronic engineering from Rajshahi University of Engineering and Technology, Bangladesh in 2005. He is an Assistant Professor in the department of Electrical & Electronic Engineering of Pabna Science and Technology University. He is now acting as a chairman in the department of Electrical and Electronic Engineering of Pabna Science and Technology University. He is a fellow of the Institution of Engineers Bangladesh (IEB).

Third Author Galib Hasan has received his B.Sc engineering degree in the department of Electrical and Electronic Engineering from Khulna University of Engineering and Technology on March 2009. After accomplishing his degree he joined as a lecturer in the Electrical and Electronic Engineering Department of Premier University on September 2009. Now he is a lecturer in the department of Electrical and Electronic Engineering of Pabna Science & Technology University, Pabna, Bangladesh. He joined as a Lecturer in the department of Electrical and Electronic Engineering Department of Pabna Science and Technology University on September, 2010.

Fourth Author Pallab Kanti Podder, has completed his B.Sc (Hons) and Masters Degree from the Department of Information & Communication Engineering of Islamic University, Kushtia, Bangladesh. After accomplishing his Masters degree he joined as a lecturer in the Computer Science & Engineering Department of Bangladesh University, Dhaka, Bangladesh. Now he is a lecturer in the Department of Information & Communication Engineering of Pabna Science & Technology University, Pabna, Bangladesh.

Fifth Author Md. Masudur Rahman has received his B.Sc engineering degree in the department of Electronic and Communication Engineering from Khulna University of Engineering and Technology on March 2008. After accomplishing his degree he joined as a lecturer in the Electrical and Electronic Engineering Department of AUST, Bangladesh. Then he was serving as a lecturer in different universities of Bangladesh. Now he is a lecturer in the department of Electrical and Electronic Engineering of Pabna Science & Technology University, Pabna, Bangladesh. He joined as a Lecturer in the department of Electrical and Electronic Engineering Department of Pabna Science and Technology University on September, 2010.